

## Rational Modification of a Candidate Cancer Drug for Use Against Chagas Disease

James M. Kraus,<sup>‡</sup> Christophe L. M. J. Verlinde,<sup>§</sup> Mandana Karimi,<sup>||</sup> Galina I. Lepesheva,<sup>⊥</sup> Michael H. Gelb,<sup>\*,‡,†,§</sup> and Frederick S. Buckner<sup>\*,†,||</sup>

Department of Chemistry, Department of Biochemistry, Department of Medicine, University of Washington, Seattle, Washington 98195-7185, Department of Biochemistry, Vanderbilt University School of Medicine, Nashville, Tennessee 37232-0146

Received October 17, 2008

Chagas disease is one of the major neglected diseases of the world. Existing drug therapies are limited, ineffective, and highly toxic. We describe a novel strategy of drug discovery of adapting an existing clinical compound with excellent pharmaceutical properties to target a pathogenic organism. The protein farnesyltransferase (PFT) inhibitor tipifarnib, now in phase III anticancer clinical trials, was previously found to kill *Trypanosoma cruzi* by blocking sterol 14 $\alpha$ -demethylase (14DM). We rationally developed tipifarnib analogues that display reduced affinity for human PFT to reduce toxicity while increasing affinity for parasite 14DM. The lead compound has picomolar activity against cultured *T. cruzi* and is efficacious in a mouse model of acute Chagas disease.

### Introduction

Chemotherapy for Chagas disease remains inadequate 100 years after the discovery of the etiologic agent, *Trypanosoma cruzi* (*T. cruzi*). This disease is responsible for approximately 21000 deaths per year, mainly in Latin America. The only drugs accepted for clinical use are the two nitroheterocyclic compounds, benznidazole and nifurtimox, which are inadequate due to toxicity and low cure rates during the chronic stage of the disease. The lack of pharmaceutical company interest for developing anti-*T. cruzi* drugs makes Chagas one of the major “neglected” diseases of the world. Our group has pursued a strategy of “piggyback” drug discovery in which we have attempted to identify compounds for Chagas disease that are well along in clinical development for other applications. We previously reported that the protein farnesyltransferase (PFT<sup>a</sup>) inhibitor tipifarnib, in phase III clinical trials for cancer, has potent activity against *T. cruzi* in vitro (EC<sub>50</sub> = 4 nM) despite having weak activity against the isolated *T. cruzi* PFT enzyme.<sup>1</sup> Surprisingly, this compound inhibited the production of endogenous sterols in *T. cruzi* by binding to *T. cruzi* 14DM. Because tipifarnib and other PFT inhibitors have dose limiting toxicities in humans (particularly bone marrow suppression<sup>2</sup>) and because tipifarnib mediates its anti-*T. cruzi* effects by a mechanism other than blocking PFT, we directed our efforts toward the

modification of the molecule in order to reduce its PFT inhibition activity and thereby eliminate a class-associated side effect.

Tipifarnib has characteristics that make it a desirable starting point for the development of an anti-Chagas drug. First, it is orally available with a long (16 h) terminal half-life.<sup>3</sup> In cancer trials, tipifarnib is usually administered by pill twice per day. Because the majority of Chagas patients reside in resource limited settings, it is desirable that the drug be given orally. Furthermore, due to the nature of the infection (chronic tissue parasitism with a slowly dividing organism), a long course of therapy lasting weeks is likely to be necessary, which realistically can only be done with drugs administered orally. Second, tipifarnib has very little inhibitory activity against mammalian cytochrome P450 enzymes.<sup>4</sup> This is important because other 14DM inhibitors, such as ketoconazole, are fraught with problems due to inhibition of hepatic and adrenal P450 enzymes. Third, tipifarnib can be synthesized in eight steps from inexpensive starting materials, resulting in relatively low manufacturing costs. In contrast, posaconazole, which has also been studied as a potential anti-Chagas drug,<sup>5</sup> requires a synthesis of at least 16 steps.<sup>6–8</sup>

The crystal structure of human PFT bound to tipifarnib and farnesyl diphosphate [PDB 1SA4]<sup>9</sup> guided our chemistry effort to abrogate the PFT inhibition activity of this compound. We looked for small changes in tipifarnib that would disrupt PFT binding while likely minimizing the impact on the pharmacologic properties of the molecule. Of course, it was necessary to make modifications that would be tolerated for interaction with the desired biological target, *T. cruzi* 14DM. Since a crystal structure for this enzyme has not been reported, predictions were made using a homology model based on the *Mycobacterium tuberculosis* CYP51 structure.<sup>1,10</sup> The compounds were tested for in vitro activity against rat PFT and against cultures of *T. cruzi* amastigotes (Table 1).

### Chemistry

The compounds were synthesized using modified published procedures.<sup>11–15</sup> The synthesis affords a racemic final product and our analogues were tested as the racemic mixture. Tipifarnib as tested is enantiomerically pure, the enantiomers being resolved either by chiral chromatography or crystallization as diastere-

\* To whom correspondence should be addressed. For biology (F.S.B.): phone, (206) 598-9148; fax, (206) 598-8819; E-mail, fbuckner@u.washington.edu; address, Division of Allergy and Infectious Disease, Department of Medicine, University of Washington, Campus Box 357185, Seattle WA 98195-7185. For chemistry (M.H.G.): phone, (206) 543-7142; fax, (206) 685-8665; E-mail, gelb@chem.washington.edu; address, Departments of Chemistry and Biochemistry, University of Washington, Campus Box 351700, Seattle WA 98195-1700.

<sup>†</sup> These authors contributed equally.

<sup>‡</sup> Department of Chemistry, University of Washington.

<sup>§</sup> Department of Biochemistry, University of Washington.

<sup>||</sup> Department of Medicine, University of Washington.

<sup>⊥</sup> Department of Biochemistry, Vanderbilt University School of Medicine.

<sup>a</sup> Abbreviations. PFT, protein farnesyltransferase; 14DM, lanosterol 14 $\alpha$ -demethylase (CYP51); *T. cruzi*, *Trypanosoma cruzi*; IC<sub>50</sub>, concentration of inhibitor resulting in 50% enzyme inhibition; EC<sub>50</sub>, concentration of inhibitor resulting in 50% parasite growth inhibition; C<sub>max</sub>, maximum plasma concentration; T<sub>max</sub>, time to reach maximum plasma concentration; CYP3A4, cytochrome p450 3A4 (predominantly hepatic p450 enzyme).

**Table 1.** In Vitro Test Results of Tipifarnib and Other Compounds (Numbers are Averages of Duplicate or Triplicate Determinations)

compd	mammalian PFT IC <sub>50</sub> (nM)	<i>T. cruzi</i> amastigote EC <sub>50</sub> (nM)	ratio IC <sub>50</sub> /EC <sub>50</sub>	CYP3A4 IC <sub>50</sub> (nM)
tipifarnib	0.7	6	0.1	1700
<b>2a</b>	13	23	0.6	
<b>2b</b>	17	45	0.4	
<b>2c</b>	294	21	14	1300
<b>2d</b>	300	23	13	1350
<b>2e</b>	4	12	0.3	
<b>2f</b>	485	22	230	550
<b>2g</b>	>5000 <sup>a</sup>	0.6	>8300 <sup>a</sup>	870
ketoconazole		0.3		40
posaconazole		0.3		350

<sup>a</sup> Compound **2g** was only evaluated up to 5 μM.

omeric salts. There are at least two main routes to compound **1** and its analogues **2a–g** (Chart 1). We followed a route that utilized a lithium–bromine exchange to generate a quinolin-6-yl anion nucleophile from a 6-bromo-2-methoxy-4-phenylquinoline **6a–g** to couple to an imidazol-5-yl-phenylmethanone **11a–c**<sup>15</sup> (see Scheme 1a). The alternative method (not depicted) utilizes a modified Skraup-type quinoline synthesis involving cyclization of a cinnamoylanilide followed by C-6 benzoylation and subsequent coupling of imidazole via organolithium species.<sup>11,13,14</sup> We chose the former convergent synthetic strategy because it promised to make the modifications we were interested in easier to access. The first proposed analogues (compounds **2a** and **2b**) had modifications to ring-1 of the scaffold (see Figure 1) and the requisite substituted benzoic acid precursors were commercially available. Initially, we expected to pursue more analogues containing modification at ring-1 and a range of substituted benzoic acids was available. All were predicted to afford the requisite Weinreb amide via nucleophilic addition–elimination of the acid chloride in high yield, whereas it was not clear that all conceivable benzoic acids would have the same reactivity in the benzoylation step of the Skraup method. Additionally, the method utilizing the Skraup cyclization required making the bond between the imidazole and the 6-benzoylquinoline via nucleophilic attack by *in situ* generated C-2 protected imidazol-5-yl anion nucleophile. Isomerization of the *in situ* generated imidazole is possible and was reported.<sup>11</sup> We predicted that these isomers (C-5 linked imidazole product and C-2 linked imidazole side product) would be difficult to separate. The imidazol-5-ylphenyl methanone intermediate **11a–c** was synthesized according to the published procedure.<sup>15</sup> The requisite benzoic acid precursor was converted to a benzoyl chloride, which upon reaction with *N,O*-dimethylhydroxylamine hydrochloride in the presence of base gives the Weinreb amide. Coupling to the *in situ* generated C-2 protected *N*-methylimidazol-5-yl anion gives the methanone intermediate **11a–c** on aqueous workup with 1 N HCl (see Scheme 1b).

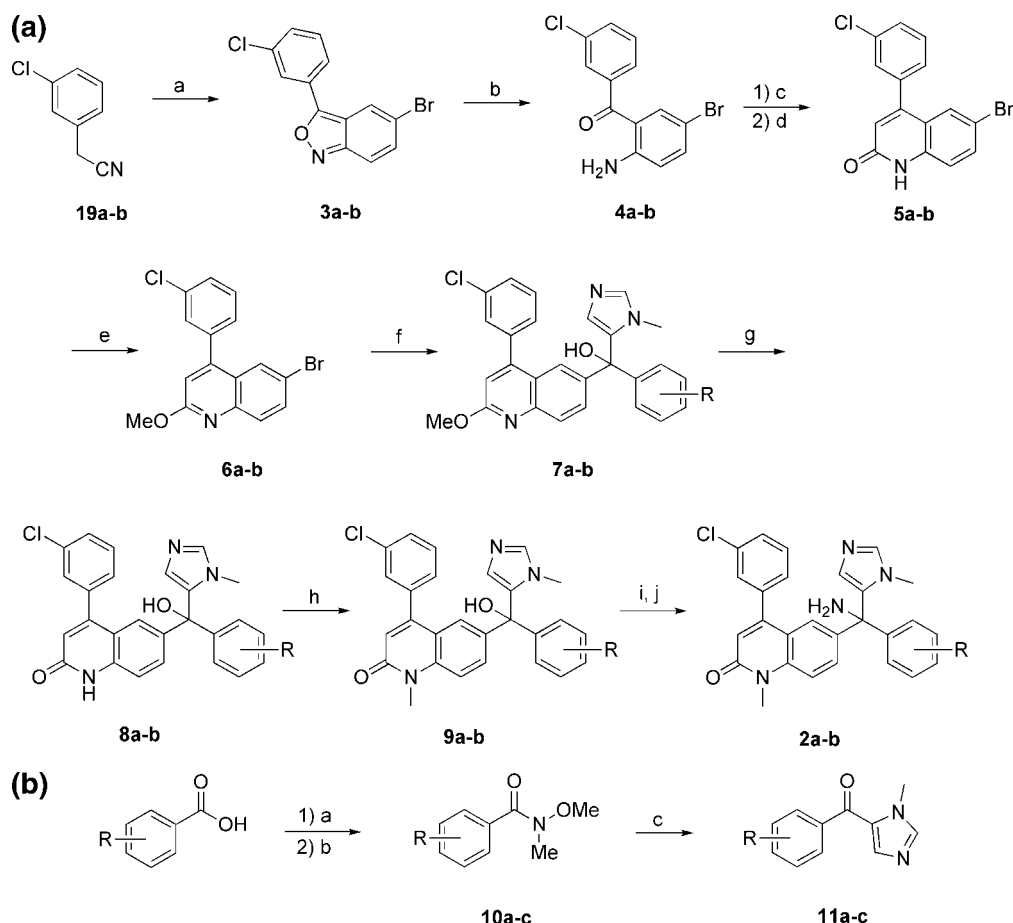
For compounds **2a,b**, the 6-bromomethoxyquinoline intermediates **6a,b** were formed via a condensation of phenylacetonitrile with nitrobenzene to form a 3-phenyl-2,1-benzisoxazole **3a,b**, which was then converted to **4a,b** by reaction with aqueous TiCl<sub>3</sub>/HCl.<sup>11,15</sup> We became interested in substitution of the ortho position of the 3-phenyl ring as a result of molecular modeling studies, compound **2c**. The requisite intermediate isoxazole **3c** had been reported via condensation of (2-methylphenyl)acetonitrile and nitrobenzene in 54% yield.<sup>16</sup> At the time, the needed phenylacetonitrile **19c** was not commercially available. Intermediate **19c** was simple to prepare in three steps using reported conditions for reduction of benzoic acid to benzyl alcohol,<sup>17</sup> conversion of the benzyl alcohol to benzyl bromide,<sup>18</sup> and substitution of bromide to cyanide<sup>19</sup> (see Scheme 2). Unfortu-

nately, we were never able to reproduce the reported 54% yield for the condensation reaction and in our hands the yield hovered at around 10%. We were very interested in this compound from a modeling standpoint, so we pushed the required material through the dismal 10% yield. Upon testing of the new analogue **2c**, we were very pleased to discover that our docking prediction was true, the installation of a simple methyl group significantly knocked down PFT affinity (around 420-fold), see Results and Discussion for details. This exciting activity led us to **2d**, which had even slightly higher selectivity, being about 430 times worse on PFT than tipifarnib. We concluded that we would like to evaluate the pharmacokinetics of these compounds in our mouse model. This required approximately 6–7 mg of product, and it did not make sense to prepare this much material via the low yielding route. We therefore sought an easier route to intermediate **4**. There are a multitude of routes to synthesize *ortho*-aminobenzophenones.<sup>20</sup> Conversion of isatoic anhydride to *ortho*-aminobenzophenone had been previously reported.<sup>12</sup> We speculated that 5-bromoisatoic anhydride could be similarly converted to the corresponding 5-bromo-2-aminobenzophenone **4c** in one step using organolithium species. We modified the protocol, using a strategy of inverse addition with 2 equiv of *in situ* generated phenyllithium to obtain intermediate **4c** in yield 71% overall yield from 5-bromoisatoic anhydride (see Scheme 3). Compounds **2a–f** were formed from intermediate **9** by substitution of alkyl chloride by gaseous ammonia. Our lead compound **2g** was formed from **9** via an acid catalyzed dehydration–etherification in methanol as solvent. It had previously been reported that higher molecular weight alcohols could be converted to the trityl type ether using catalytic amounts of *p*-toluenesulfonic acid and a Dean–Stark apparatus utilizing the benzene–water azeotrope to remove water.<sup>21</sup> We simply dissolved the starting material in methanol and heated to reflux in the presence of catalytic amounts of tosic acid. This led to conversion of **9** to **2g** in 75% isolated yield on the gram scale. All of the analogues that we prepared are racemates. Our plan is to go forward with preclinical development of these compounds as racemates.

## Results and Discussion

Molecular modeling suggested that modifications to ring-1 (Figure 1) would partially displace tipifarnib from the PFT active site. When tested, the addition of a 3-methyl to the tipifarnib ring-1, compound **2a**, gave rise to a 19-fold increase in IC<sub>50</sub> (to 13 nM) on rat PFT compared to tipifarnib. A slightly larger effect on PFT inhibition (IC<sub>50</sub> 17 nM) was observed by substituting a naphthyl group at the ring-1 position in compound **2b**. These initial analogues showed the desired trend, but the decrease in PFT inhibition was accompanied by a decrease in activity against the parasites. To achieve the desired result, we next explored modifications on ring-2 of tipifarnib (Figure 1). Introduction of a 2-methyl group on this ring (**2c**) was predicted to be detrimental for binding to human PFT by causing steric clash with the molecular surface of the binding pocket (Figure 2a). Ring-2 of tipifarnib points to a hydrophobic pocket near the entrance to the active site in the 14DM model. We predicted that tipifarnib does not fill this pocket, leaving room for a methyl group (**2c**, Figure 2b). Specifically, compound **2c** displays a 420-fold decrease in PFT inhibition with an IC<sub>50</sub> of 294 nM on mammalian PFT and only minor reduction in activity against *T. cruzi* amastigotes. A more substantial change of replacing the tipifarnib ring-2 with a naphthyl group in **2f** further knocked down PFT inhibition (IC<sub>50</sub> 485 nM) while retaining anti-*T. cruzi* activity. All along we adhered to a “piggyback” strategy, using

**Scheme 1.** (a) Synthesis of Tipifarnib Analogues from Phenylacetonitrile. (b) Synthesis of (Imidazol-5-yl)phenylmethanone Intermediate (11)



<sup>a</sup> (a) *p*-Bromonitrobenzene, NaOH, MeOH, 10–50%. (b) TiCl<sub>3</sub>, H<sub>2</sub>O/THF, rt, 62%. (c) Ac<sub>2</sub>O, toluene, reflux. (d) *t*-BuOK, DME, 20 °C, 66% (2 steps). (e) BF<sub>4</sub>OMe<sub>3</sub>, DCM, 63%. (f) (i) *n*-BuLi, THF, –78 °C; (ii) (11a–c) 60%. (g) 6 N HCl, THF, reflux, 6 h, 60%. (h) CH<sub>3</sub>I, NaOH, BTEAC, THF, rt, 66%. (i) SOCl<sub>2</sub>, neat, 12 h. (j) NH<sub>3</sub>, THF, rt, 52% (2 steps). (b) (a) SOCl<sub>2</sub>, neat, rt. (b) CH<sub>3</sub>ONHCH<sub>3</sub>, pyridine, DCM, 90% (2 steps). (c) *N*-Methylimidazole; (i) *n*-BuLi, THF, –78 °C; (ii) Et<sub>3</sub>SiCl, –78 °C; (iii) *n*-BuLi, THF, –78 °C, 77%.

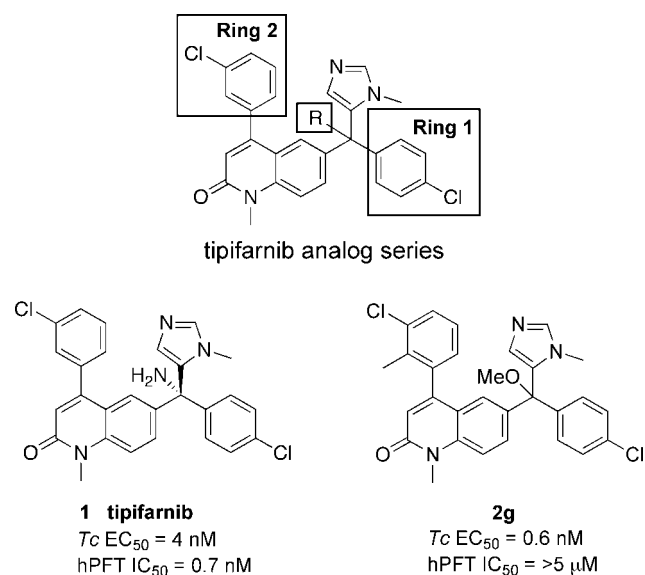


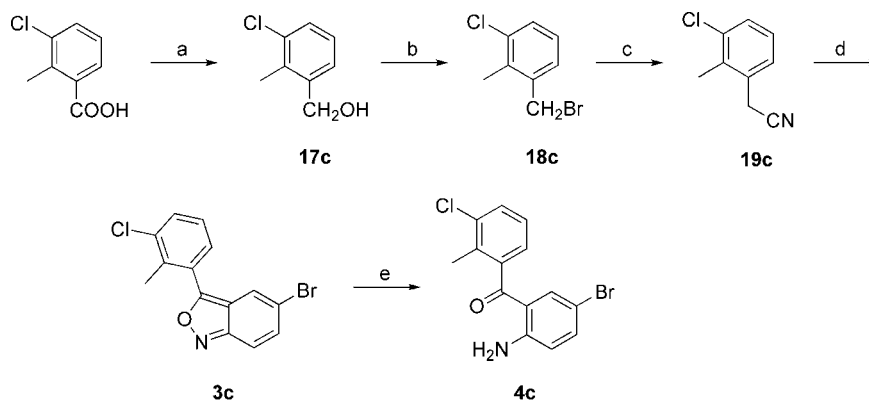
**Figure 1.** Tipifarnib analogue series ring numbering, tipifarnib and compound **2g**.

a philosophy that smaller changes would be better, if made in the right places, because the parent compound, compound **1** had excellent pharmaceutical properties to begin with and big

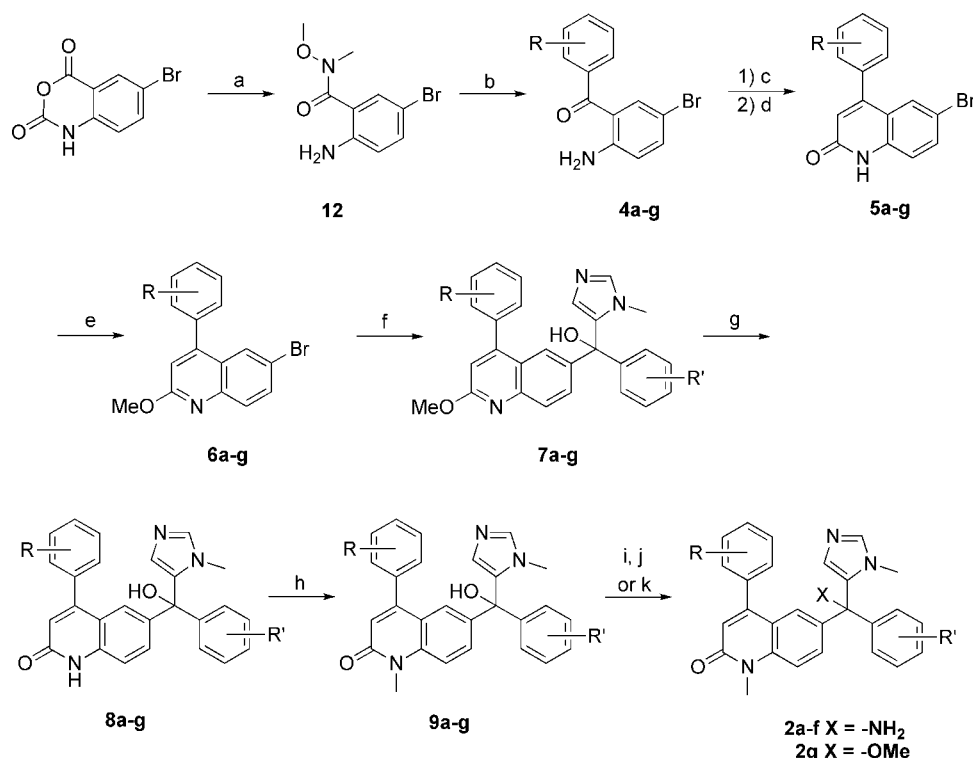
changes might have a big effect on pharmacokinetics or toxicity. Because compound **2c** had such high selectivity from the installation of simple methyl group, we decided to proceed with this basic structure.

The amino group of tipifarnib makes a water-mediated H-bond to a phosphate oxygen of farnesyl diphosphate in the active site of mammalian PFT.<sup>9</sup> Our homology model of *T. cruzi* demethylase predicted that H-bonding to this amino group is not important for binding in 14DM,<sup>1</sup> so we substituted NH<sub>2</sub> for OMe to arrive at **2g**. Relative to tipifarnib, this compound resulted in a ~10-fold increase in potency against *T. cruzi* amastigotes while having further reduced activity against PFT (IC<sub>50</sub> > 5000 nM). We speculate that this improved cellular activity may be due to increased affinity for 14DM or increased cellular permeability. Using recombinant *T. cruzi* 14DM reconstituted in vitro with P450 reductase, we showed that **2c**, **2f**, and **2g** bind to Tc14DM with equilibrium dissociation constants much less than minimum concentration of the enzyme required in the assay (1 μM, see Supporting Information). In the same conditions tipifarnib, **2c**, **2f**, and **2g** do not inhibit the human 14DM (see Supporting Information).

The potency of **2g** against *T. cruzi* cultures puts it in the same league as the most potent (antifungal) azoles, ketoconazole and posaconazole (Table 1). Therefore, we moved ahead with **2g** as the lead for additional in vivo studies beginning with pharmacokinetic studies in mice. Figure 3a shows that **2g** has

**Scheme 2.** Synthesis of 3-Chloro-2-methylphenylacetonitrile Intermediate<sup>a</sup>

<sup>a</sup> (a) LAH, THF, quant.; (b) PBr<sub>3</sub>, DCM, 90%; (c) NaCN, DMSO, 85%; (d) *p*-BrPhNO<sub>2</sub>, NaOH, MeOH, 10%; (e) TiCl<sub>3</sub>, H<sub>2</sub>O/THF, rt, 50% (4% overall).

**Scheme 3.** Synthesis of Tipifarnib Analogues from 5-Bromoisoatonic anhydride<sup>a</sup>

<sup>a</sup> (a) CH<sub>3</sub>ONHCH<sub>3</sub> HCl, pyridine, DCM, 83%. (b) RPhBr (2 equiv), *n*-butyllithium (2 equiv), THF, 85%. (c) Ac<sub>2</sub>O, toluene, reflux. (d) *t*-BuOK, DME 20 °C, 66% (2 steps). (e) BF<sub>4</sub>OMe<sub>3</sub>, DCM, 63%. (f) (i) *n*-BuLi, THF, -78 °C; (ii) (11a–c), 60%. (g) 6 N HCl, THF, reflux, 60%. (h) CH<sub>3</sub>I, NaOH, BTEAC, THF, rt, 66%. (i) SOCl<sub>2</sub>, neat, 12 h. (j) NH<sub>3</sub>, THF, rt, 52% (2 steps). (k) tosic acid (1 equiv + cat.), MeOH, reflux, 75%.

a very similar pharmacokinetic profile to tipifarnib in mice, with peak serum concentrations ( $C_{\max}$ ) of 5–7  $\mu\text{M}$  and an elimination half-life ( $T_{1/2}$ ) of  $\sim 4$  h. On the basis of these results, we designed an efficacy study using **2g** in a mouse model of Chagas disease (Figure 3b). In this model, a parasite infection is first established for 7 days and then **2g** is administered by oral gavage over a 20 day period (see Supporting Information). Control mice given only the vehicle developed steadily rising parasitemia and death by day 16 postinfection. Compound **2g** suppressed parasitemia to microscopically undetectable levels, similar to the effect of the control drug benznidazole. Interestingly, tipifarnib only delayed the development of high parasitemia by 3–4 days and did not protect the mice from death. This is probably due to the 10-fold lower potency of tipifarnib on *T. cruzi* compared to **2g**, but it could also be related to other factors such as tissue distribution of the compounds. One mouse in the **2g** group died

after the end of treatment. This was not due to inadequate parasitologic clearance but appeared to be related to a physical complication from receiving multiple gavage treatments. The other four mice in the group remained healthy and did not experience apparent adverse effects from the **2g** treatment. The benznidazole treated mice also tolerated the treatment without apparent adverse effects. At 100 days postinfection, parasites were microscopically undetectable in the blood. At day 103, the mice were sacrificed, exsanguinated, and blood cultures were set up to test for parasitologic cure. All four surviving **2g**-treated mice had positive parasite blood cultures and three of six benznidazole-treated mice had positive blood cultures. This indicates that neither compound was completely curative using this treatment regimen. There are numerous animal models of the disease in the literature involving different strains of *T. cruzi* as well as various drug dosing schedules and timelines.<sup>5,22–26</sup>



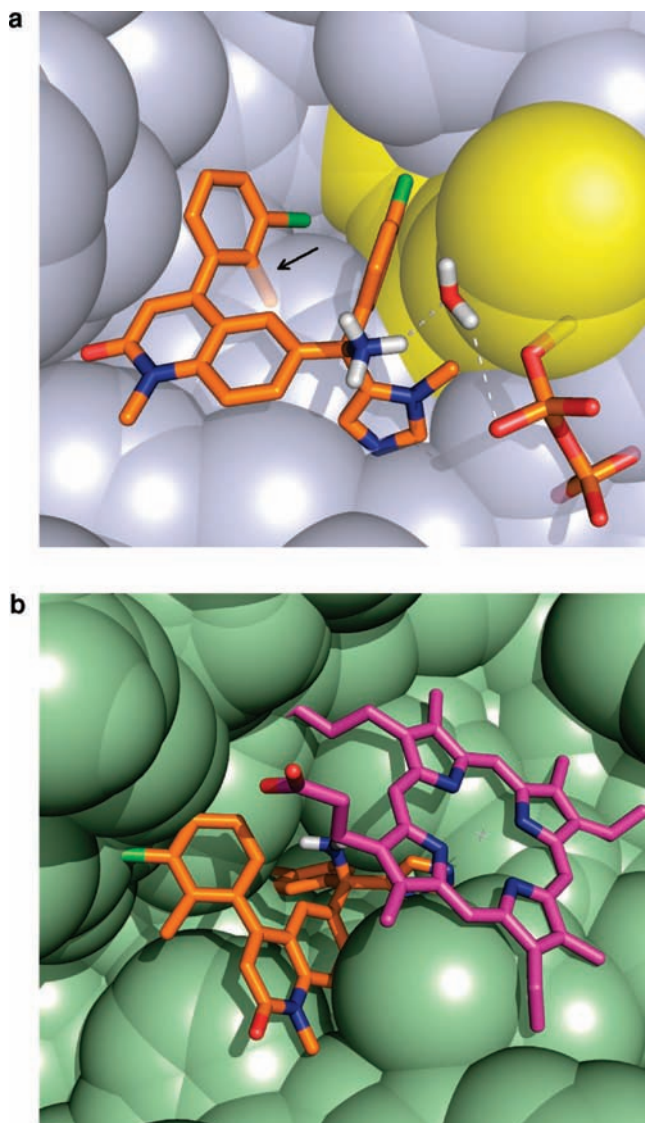


**Figure 2.** (a) Mammalian PFT depicted with bound compound **2c**. Compound **2c** is depicted instead of the lead **2g** in order to show water-mediated hydrogen bonding between the ammonium group of tipifarnib or compound **2c** and the  $\beta$ -phosphate oxygen, which are shown in dotted lines. Compound **2c**, bridging water, and the diphosphate of farnesyl diphosphate are rendered as sticks. The prenyl chain is shown as yellow spheres. All van der Waal surfaces are displayed as doubled-radius surfaces to show ligand contacts. The superimposed arrow indicates the clash between the 2-methyl group of compound **2c** and the PFT surface. PFT  $\alpha$ -subunit and residues R291 to K294 have been removed from the picture for clarity. (b) *T. cruzi* 14DM with bound compound **2c** and heme (both displayed as sticks) showing the accommodation of the inhibitor's 2-methyl group. An 11 Å sphere around the inhibitor is depicted and residues P93-N102, F103-T109, and F386-V406 removed from figure for clarity. All van der Waal surfaces are displayed as doubled-radius surfaces to show ligand contacts.

We chose the model involving dosing for 20 days because it is so widely used.<sup>5,22,23,25,26</sup> As with other chronic infections, it is possible that combination chemotherapy may be necessary to completely eliminate *T. cruzi* from the human host.

The tipifarnib analogues display poor inhibition of the hepatic cytochrome P450 enzyme, CYP3A4, compared to the azole antifungal drugs (Table 1). This indicates that the tipifarnib analogues are likely to produce fewer problems with drug–drug interactions than the azole class of antifungal drugs, which have also been investigated as anti-*T. cruzi* agents via inhibition of sterol 14 $\alpha$ -demethylase.

The new tipifarnib analogues were shown to have low cytotoxicity against a panel of mammalian cells with EC<sub>50</sub> values > 5  $\mu$ M for all compounds against five different types of cell lines (data not shown).

The best compound, **2g**, did not have apparent toxicity in mice when dosed at 50 mg/kg twice per day. This compound also appears to retain the desirable properties of tipifarnib in terms of a good pharmacokinetic profile when administered orally (in mice) and demonstrating weak inhibition of the human CYP3A4 enzyme in vitro.

## Conclusions

We describe a novel strategy of drug discovery in which we modified an existing clinical cancer compound with excellent pharmaceutical properties, compound **1**, to use as an antiparasitic. We previously discovered that this compound has activity against two enzymes, an off-target human PFT enzyme and *T. cruzi* lanosterol 14 $\alpha$ -demethylase. Small changes to the structure of compound **1** led to complete elimination of PFT inhibitory activity and simultaneously increased activity against *T. cruzi*. Our best compound, **2g**, is orally available, inexpensive to produce and extremely potent, showing activity at picomolar concentrations in vitro. In a mouse model of the disease, **2g** showed complete suppression of parasitemia, microscopically, and efficacy comparable to the principle clinical therapeutic, benznidazole, which has toxic side effects. Removal of the PFT inhibitory activity in this group of compounds is expected to eliminate class-associated side effects inherent to PFT inhibitors. **2g** is one of the most potent *T. cruzi* compounds ever reported, and we are optimistic that a compound such as **2g** is extremely promising for further development as a clinical candidate for Chagas disease.

## Experimental Methods

**Molecular Modeling.** We made use of the crystal structure of Rat PFT in complex with tipifarnib<sup>9</sup> and the homology model of the *T. cruzi* CYP51 in complex with tipifarnib, based on the *Mycobacterium tuberculosis* enzyme structure, described earlier in detail,<sup>1</sup> for all molecular modeling. Design and docking studies were carried out with the FLO/QXP program suite, version 0602.<sup>27</sup> In each case amino acid residues within 11 Å of tipifarnib were included in the binding site model for Metropolis Monte Carlo searches and energy minimization procedures. Details of the procedures were earlier described for human PFT.<sup>1</sup> Figures of structural models were created using PyMOL (www.pymol.org).

**PFT Enzyme Assay.** Expression and purification of recombinant rat PFT in *Sf9* cells was reported previously.<sup>28</sup> Compounds were screened against rat PFT by a <sup>3</sup>H-Scintillation Proximity Assay (SPA; TRKQ7010; Amersham Biosciences Corporation, Piscataway, NJ). The experiments were performed as described elsewhere<sup>29</sup> with the following modifications. Rat PFT assays were carried out in buffer (pH 7.5, 50 mM HEPES, 30 mM MgCl<sub>2</sub>, 20 mM KCl, 5 mM dithiothreitol, 0.01% Triton X-100), 1  $\mu$ M human lamin B carboxy-terminus peptide (biotin-YRASNRSCAIM), and 1  $\mu$ Ci [<sup>3</sup>H]farnesyl diphosphate (15–20 Ci/mole; Amersham) in a total volume of 50  $\mu$ L, which included 1  $\mu$ L of PFT inhibitor solution in dimethylsulfoxide (DMSO) and 10 ng of purified rat PFT. The reaction mixtures were incubated at 37 °C for 20 min and terminated by addition of 70  $\mu$ L of assay STOP solution (Amersham) and 5  $\mu$ L SPA beads. The assay mixture was incubated at room temperature for 30 min. The assay results were counted on a Chameleon 425-104 multilabel plate counter (Hidex Oy) that detected the photons emitted by the scintillation beads bound to biotin-peptide-[<sup>3</sup>H]farnesyl. The inhibitor concentration that caused 50% PFT inhibition (IC<sub>50</sub>) was determined by nonlinear regression analysis of a plot of percent enzyme inhibition versus log of

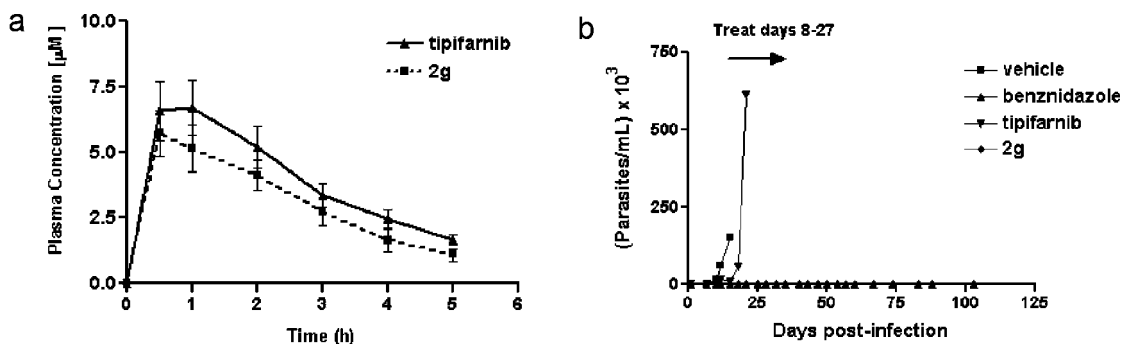


**Figure 3.** Pharmacokinetics and efficacy of tipifarnib and 2g in mice. (a) Plasma levels were monitored following a single oral dose of 50 mg/kg in uninfected mice. Plotted values are an average of three mice for both tipifarnib and compound 2g. (b) Efficacy was monitored by measuring parasitemia in *T. cruzi* infected mice receiving treatment with tipifarnib (50 mg/kg twice daily), compound 2g (50 mg/kg twice daily), vehicle (twice per day), or benznidazole (100 mg/kg once daily). Treatments were administered by oral gavage for 20 consecutive days beginning on day 8 postinfection with *T. cruzi* trypomastigotes. Vehicle treated mice (negative control) were all dead by day 16 postinfection.

inhibitor concentration. Curves were fit to a variable slope sigmoidal dose–response curve using GraphPad Prism 3.0 (www.graphpad.com).

***T. cruzi* Growth Inhibition Assay.** Compounds were screened against the  $\beta$ -galactosidase expressing Tulahuen strain of *T. cruzi* in 96-well tissue culture plates as described previously.<sup>30</sup>

**Mammalian Cell Growth Inhibition Assays.** Compounds were screened for cytotoxicity against five different mammalian cell lines representing different tissue types: HT-1080 (human fibrosarcoma), SF-539 (human neural cells), HCC-2998 (human adenocarcinoma), THP-1 (human macrophage), and CRL-8155 (human lymphocyte). All cell lines were purchased from American Tissue Culture Collection. Cells were grown in the presence of compounds for 48 h before growth was quantified using Alamar Blue (Alamar Biosciences Inc., Sacramento, CA). Compounds were tested at final concentrations of 25, 12.5, 6.25, 3.13, 1.56, and 0.78  $\mu$ M.

**CYP3A4 Inhibition Assay.** Inhibition of recombinant human CYP3A4 enzyme was determined using a commercial kit (CYP3A4/BFC High Throughput Inhibitor Screening Kit) following the manufacturer's instructions (GenTest, Inc.).

**Pharmacokinetic Studies in Mice.** Compounds were suspended at 10 mg/mL in 20% (w/v) Trappsol hydroxypropyl  $\beta$ -cyclodextrin (pharmaceutical grade) (CTD, Inc.) and administered to BALB/c mice (7–8 week females weighing approximately 20 g) by oral gavage in a volume of 100  $\mu$ L. Thus, the mice received a dose of 50 mg/kg. At timed intervals, 40  $\mu$ L of tail blood was collected in heparinized capillary tubes. Plasma was separated by centrifugation and frozen for later analysis. After thawing, 10  $\mu$ L of plasma was mixed with 11  $\mu$ L of acetonitrile containing 100 pmols compound 2e as an internal standard. The mixture was vortexed, then mixed with 30  $\mu$ L of extraction solvent composed of 80% acetonitrile and 20% H<sub>2</sub>O by volume. This was centrifuged at 13200 rpm for 10 min at which time most of the supernatant was transferred to a new tube and dried down to a solid. To determine response factors, 10  $\mu$ L of fresh plasma (containing no drug) was obtained and spiked with 100 pmols of analyte and then mixed with 11  $\mu$ L of acetonitrile containing 100 pmols of compound 2e. This was similarly vortexed, mixed with 30  $\mu$ L extraction solvent, centrifuged at 13200 rpm for 10 min, at which time most of the supernatant was transferred to a new tube and dried down to a solid. Samples were reconstituted in 50  $\mu$ L of a mixture of 50% acetonitrile and 50% water by volume. Concentrations were determined by liquid chromatography–mass spectrometry using an Agilent (Palo Alto, CA) HP 1100 chromatograph and an Esquire-LC (Bruker, Billerica, MA) electrospray ion trap mass spectrometer. Reversed-phase LC separation was performed using an Agilent Zorbax SB-C18 (3.5  $\mu$ m, 2.1 mm  $\times$  100 mm) with a mobile phase consisting of water/5% acetonitrile/1% acetic acid (solvent A) and acetonitrile/1% acetic acid (solvent B). Mobile phase gradient went from 10% solvent B to 64% solvent B over 9 min with a flow rate of 0.2 mL/min, then flow rate was increased to 0.35 mL/min with a gradient from 64% solvent B to 100% over 5 min. Compounds were quantified by integration of

the area of each peak in an extracted ion chromatogram. Quantification was performed with Bruker QUANTANALYSIS software using response factors established for the internal standard.

**Efficacy Studies in Mice.** BALB/c mice (7–8 week females) were infected with  $5 \times 10^3$  *T. cruzi* trypomastigotes (Tulahuen strain) by subcutaneous injection. By 7 days postinfection, every mouse had microscopically observable parasites on slides of peripheral blood. On day 8 postinfection, mice (in groups of five or six) began receiving treatments by oral gavage. For tipifarnib and 2g, mice were initially dosed at 100 mg/kg twice per day (days 8–13), but some weight loss was observed, so the dose was reduced to 50 mg/kg twice per day for days 14–27. The benznidazole group received this drug at 100 mg/kg once per day (days 8–27). The control group received the vehicle (20% (w/v) Trappsol hydroxypropyl  $\beta$ -cyclodextrin (pharmaceutical grade) (CTD, Inc.)), in a volume of 100  $\mu$ L twice per day. Parasitemia was monitored by placing 5  $\mu$ L of tail blood under a coverslip and counting 50 high-powered fields. Mice that were premonitory from progressive infection were euthanized. All surviving mice were sacrificed on day 103 postinfection and  $\sim$ 500  $\mu$ L of blood from cardiac puncture was taken for culture in liver-infusion tryptone medium plus 10% heat-inactivated fetal bovine serum, penicillin, and streptomycin.<sup>31</sup> The culture was incubated at 28  $^{\circ}$ C and checked weekly (for 8 weeks) for outgrowth of *T. cruzi* epimastigotes.

**Chemistry.** Starting materials were purchased from Aldrich, Acros, Alfa-Aesar, EMD, Fisher, Lancaster, Mallinckrodt, TCI-America, or VWR and used without further purification, unless otherwise specified. *N*-methylimidazole (M50834) was purchased from Sigma-Aldrich and distilled at reduced pressure (10 mm Hg, bp: 67–69  $^{\circ}$ C) after being stirred over sodium at room temperature overnight. Solvents were purified using a J. C. Meyer type solvent dispensing system utilizing Al<sub>2</sub>O<sub>3</sub> and/or copper cartridges, depending on the particular solvent. Nitrogen gas used in reactions requiring an inert atmosphere was house supplied nitrogen run through Dry-Rite desiccant. Glassware for distillation and critical reactions was flame dried under vacuum or dried in an oven. Silica was EMD Silica Gel 60, 40–63  $\mu$ m (11567-1). TLC plates were aluminum backed EMD Silica Gel 60 F<sub>254</sub> (5554/7). NMR spectra were recorded on a Bruker Avance AV300. ESI-MS were recorded on a Bruker Esquire ion trap mass spectrometer. The synthesis of compound 2g is described and compounds 2a–f were prepared in an analogous fashion using the corresponding commercially available starting materials. Purification of final compounds was by reverse phase HPLC utilizing octadecylsilane stationary phase and a water-to-methanol gradient with 0.08% v/v trifluoroacetic acid, (TFA). HPLC was a Varian Pro-Star fitted with YMC Pack-ODS-A 2 cm  $\times$  10 cm column running at 12 mL/min using an excitation wavelength of 254 nm. All tested target compounds possessed a purity of  $\geq$ 95% as verified by HPLC.

**2-Amino-5-bromo-*N*-methoxy-*N*-methylbenzamide (12).** A 2 L flask was charged with 10.0 g (41.3 mmol) 5-bromoisatoic anhydride (242.03 g/mol) and 6.0 g (61.5 mmol) *N,O*-dimethyl-



hydroxylamine hydrochloride (97.54 g/mol). The solids were suspended in 150 mL of anhydrous  $\text{CH}_2\text{Cl}_2$  and stirred rapidly. Then 15.0 mL pyridine (186 mmol) was added slowly, and the mixture was allowed to stir overnight. The crude mixture was partitioned between  $\text{CHCl}_3$  and water. The organic phase was washed with brine and dried with anhydrous  $\text{MgSO}_4$ . Solvents were removed under reduced pressure to produce a golden-colored oil which crystallized upon standing. Product was triturated with hexanes, filtered, and then used without further purification; 8.3 g lightly colored crystalline **12** was produced, 83% yield.  $^1\text{H NMR}$  (300 MHz,  $\text{CDCl}_3$ ,  $\delta$ ): 7.52 (d,  $J = 2.4$  Hz, 1H), 7.28 (dd,  $J = 2.4$  Hz, 8.1 Hz 1H), 6.61 (d,  $J = 8.7$  Hz, 1H), 4.69 (s (broad), 2H), 3.61 (s, 3H), 3.36 (s, 3H). ESI-MS  $m/z$  283.1 ( $\text{M} + \text{Na}^+$ ) $^+$ . MW: 259.10 g/mol.

**(2-Amino-5-bromophenyl)(3-chloro-2-methylphenyl)methanone (4g)**. A 250 mL flask was flame dried, charged with a stirbar, and sealed with a new rubber septum. 2-Bromo-6-chlorotoluene (6 mL, 45.9 mmol) was added to the flask and dissolved in 60 mL of anhydrous THF under an atmosphere of dry nitrogen. The solution was stirred for about 5 min and then cooled to  $-78^\circ\text{C}$  with a dry ice acetone bath, and then stirred for about 10 min. Then 18 mL (45.9 mmol, 1 equiv) of *n*-butyllithium (2.5 M in hexanes) was added dropwise at a rate such that temperature of the reaction remained close to  $-78^\circ\text{C}$ , as indicated by the slow sublimation of  $\text{CO}_2$ . The solution was allowed to stir for 20 min. A separate flask was flame dried and fitted with a stir-bar and septum. 2-Amino-5-bromo-*N*-methoxy-*N*-methylbenzamide **12** (5.95 g, 22.95 mmol, 0.5 equiv) was added and dissolved in 60 mL of anhydrous THF. After stirring for about 5 min, this solution was transferred dropwise by cannula to the flask containing the in situ generated aryllithium. The solution was allowed to stir at this temperature for 2 h, at which time the cooling bath was removed, allowing the flask to rise to room temperature. Then 50 mL of 1 M aqueous HCl was added and the biphasic mixture was allowed to stir for 30 min. Crude product was partitioned between  $\text{CHCl}_3$  and water. The organic phase was washed three times with saturated, aqueous  $\text{NaHCO}_3$ , and then separated and dried with  $\text{MgSO}_4$ . Solvents were removed under reduced pressure to produce an orange-brown colored oil. This was purified on silica with 20% EtOAc/hexanes to produce 6.3 g of yellow crystalline **4g**, yield 85%.  $^1\text{H NMR}$  (300 MHz,  $\text{CDCl}_3$ ,  $\delta$ ): 7.47 (d,  $J = 7.8$  Hz, 1H), 7.36 (dd,  $J = 8.7$  Hz, 2.1 Hz, 1H), 7.25 (d,  $J = 2.1$  Hz 1H), 7.21 (m, 2H), 7.11 (d,  $J = 7.5$  Hz 1H), 6.64 (d,  $J = 8.7$  Hz, 1H), 6.49 (s (broad), 2H), 2.27 (s, 3H). ESI-MS  $m/z$  324.3 ( $\text{M} + \text{H}^+$ ) $^+$ . MW: 324.60 g/mol.

**6-Bromo-4-(3-chloro-2-methylphenyl)quinolin-2(1H)-one (5g)**. A 250 mL flask was fitted with a stir-bar and 11.9 g of **4g**. A water condenser was attached. Then 50 mL of anhydrous toluene was added and 24.3 mL (257 mmol, 7 equiv) acetic anhydride was added dropwise, rapidly. The solution was heated to reflux for 6 h, at which time the volatiles were removed under reduced pressure. Toluene was added and removed at reduced pressure two more times. The crude product was set aside. A separate flask was fitted with a stir-bar and a septum and loaded with 24.7 g (220 mmol, 6 equiv) of 95% tBuOK powder. This was suspended in 120 mL of 1,2-dimethoxyethane (DME) and stirred for about 10 min. The temperature was lowered to  $0^\circ\text{C}$ . The crude product set aside previously was dissolved in 45 mL of 1,2-dimethoxyethane and then transferred dropwise by cannula to the flask containing the tBuOK suspension. The color of the solution changed to yellow, and the mixture was allowed to stir under an inert atmosphere overnight. DME solvent was removed at reduced pressure and the resulting paste was suspended in approximately 300 mL water. The solid was collected by filtration and used at the next step without purification. 8.4 g (24.10 mmol) of **5g** was produced as a fluffy, white solid, yield 66%.  $^1\text{H NMR}$  (300 MHz,  $\text{CDCl}_3$ ,  $\delta$ ): 7.62 (dd,  $J = 8.7$  Hz, 1.8 Hz, 1H), 7.53 (d,  $J = 7.8$  Hz, 1H), 7.39 (d,  $J = 8.7$  Hz, 1H), 7.30 (m, 1H), 7.21 (d,  $J = 1.8$  Hz, 1H), 7.11 (d,  $J = 7.2$  Hz, 1H), 6.62 (s, 1H), 2.17 (s, 3H). ESI-MS  $m/z$  348.3 ( $\text{M} + \text{H}^+$ ) $^+$ . MW: 348.62 g/mol.

#### **6-Bromo-4-(3-chloro-2-methylphenyl)-2-methoxyquinoline (6g)**

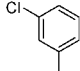
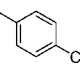
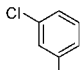
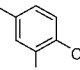
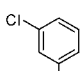
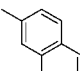
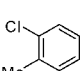
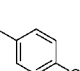
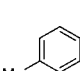
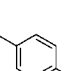
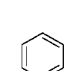
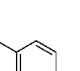
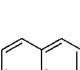
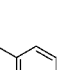
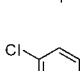
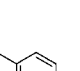
A flame dried 25 mL flask was fitted with a stir-bar and charged with 500 mg (1.43 mmol) of **5g** and 423 mg (2.86 mmol, 2 equiv)  $\text{BF}_3\text{OEt}_2$  and then sealed with a septum. The solids were suspended in 5.5 mL of anhydrous  $\text{CH}_2\text{Cl}_2$  and stirred for 20 h, at which time 5.5 mL of 1 M aqueous NaOH was added. The mixture was stirred for about 3 h, then partitioned between  $\text{CHCl}_3$  and water, and the organic was washed three times with brine and then dried with  $\text{MgSO}_4$ . Solvents were removed under reduced pressure to produce a clear yellow oil, which crystallized upon standing. This was purified on silica with 50:50  $\text{CH}_2\text{Cl}_2$ :hexane to produce 329 mg of **6g** as a flaky yellow-green solid, yield 63%.  $^1\text{H NMR}$  (300 MHz,  $\text{CDCl}_3$ ,  $\delta$ ): 7.79 (d,  $J = 9.0$  Hz, 1H), 7.69 (dd,  $J = 8.7$  Hz, 2.3 Hz, 1H), 7.50 (dd,  $J = 7.8$  Hz, 1.2 Hz, 1H), 7.40 (d,  $J = 2.1$  Hz, 1H), 7.26 (m, 1H), 7.09 (dd,  $J = 7.5$  Hz, 1.2 Hz, 1H), 6.77 (s, 1H), 4.10 (s, 3H), 2.08 (s, 3H). ESI-MS  $m/z$  362.3 ( $\text{M} + \text{H}^+$ ) $^+$ . MW: 362.65 g/mol.

**4-Chloro-*N*-methoxy-*N*-methylbenzamide (10c)**. 4-Chlorobenzoic acid (20.0 g, 0.128 mols, 156.57 g/mol) was placed in a 500 mL round-bottomed flask. Thionyl chloride (120 mL) was added, and the mixture was refluxed overnight. Thionyl chloride was removed under reduced pressure to produce a red-colored oil. Anhydrous toluene was added and then removed under reduced pressure two times. The crude product was dissolved in 200 mL anhydrous dichloromethane (DCM). Then 13.73 g (0.140 mols) *N,O*-dimethylhydroxylamine·HCl (97.54 g/mol) was added, and 52 mL (0.640 mols) anhydrous pyridine was added over a period of 10 min. The reaction was stirred under nitrogen at room temperature overnight. Volatiles were removed under reduced pressure. Solid was partitioned between  $\text{CHCl}_3$  and water. The organic phase was washed with brine and then collected and dried over anhydrous magnesium sulfate. The solvents were removed to produce a red-colored oil, which was purified on silica with 5% MeOH/ $\text{CH}_2\text{Cl}_2$  as eluent; 22.9 g produced, yield 90%.  $^1\text{H NMR}$  (300 MHz,  $\text{CDCl}_3$ ,  $\delta$ ): 7.66 (d,  $J = 8.4$  Hz, 2H), 7.38 (d,  $J = 8.4$  Hz, 2H), 3.54 (s, 3H, -OMe), 3.36 (s, 3H, -NMe). ESI-MS  $m/z$  200.4 ( $\text{M} + \text{H}^+$ ) $^+$ . MW: 199.63 g/mol.

#### **(4-Chlorophenyl)(1-methyl-1*H*-imidazol-5-yl)methanone (11c)**

A flame-dried 125 mL round-bottomed flask was charged with a stir bar and overpressurized with dry nitrogen gas and 3.0 mL (37.6 mmol) freshly distilled *N*-methylimidazole (82.11 g/mol, 1.035 g/mL). The flask was sealed with a new rubber septum, and 30 mL anhydrous THF was added. The solution was stirred for about 10 min, and then the temperature was lowered to  $-78^\circ\text{C}$  and stirred for an additional 10 min. Then 16.2 mL (41.3 mmol) freshly titrated *n*-butyl lithium (2.5 M in hexanes) was added dropwise through the septum over a period of 10 min under an overpressure of dry nitrogen. A slight color change to pale yellow was observed. This was allowed to stir at this temperature for 45 min, and then 6.3 mL (37.6 mmol) 99% chlorotriethylsilane ( $\text{Et}_3\text{SiCl}$ ) was added dropwise over 5 min. The reaction was allowed to stir for 1 h at  $-78^\circ\text{C}$ , at which point 15.0 mL (37.6 mmol) freshly titrated *n*-butyl lithium (2.5 M in hexanes) was added dropwise through the septum over a period of 10 min and allowed to stir at  $-78^\circ\text{C}$  for an additional 45 min. A separate flask was flame-dried and charged with 5.0 g (25.1 mmol) Weinreb amide **10c** (199.63 g/mol) and sealed. Then 15 mL of anhydrous THF was added and the mixture was stirred at room temperature for 10 min, and then at the appropriate time, transferred via cannula to the flask containing the in situ generated C-2 triethylsilyl protected *N*-methylimidazole at a slow rate to maintain low temperature as indicated by the slow sublimation of  $\text{CO}_2$ . The mixture was left to stir overnight and became a deep-red color. The reaction was quenched by the addition of 1 M HCl until the pH of the aqueous phase was no longer basic, as indicated by litmus paper, and then allowed to stir for one hour. The pH of the aqueous phase was adjusted to above 8 with 1.5 M NaOH, and the mixture was partitioned between  $\text{CHCl}_3$  and water. The organic phase was washed with brine and dried with anhydrous  $\text{MgSO}_4$ . Solvents were removed under reduced pressure to produce a reddish solid. Product was purified by recrystallization from  $\text{CH}_2\text{Cl}_2$  to produce 4.24 g of fluffy golden crystals, 76.6% yield.

**Chart 1.** Structures of Tipifarnib **1** and Tipifarnib Analogues **2a–g**

Compound	Ring 2	Ring 1	R
<b>1</b>			-NH <sub>2</sub>
<b>2a</b>			-NH <sub>2</sub>
<b>2b</b>			-NH <sub>2</sub>
<b>2c</b>			-NH <sub>2</sub>
<b>2d</b>			-NH <sub>2</sub>
<b>2e</b>			-NH <sub>2</sub>
<b>2f</b>			-NH <sub>2</sub>
<b>2g</b>			-OMe

<sup>1</sup>H NMR (300 MHz, CDCl<sub>3</sub>, δ): 7.83 (d, *J* = 8.4 Hz, 2H), 7.68 (s, 1H), 7.59 (s, 1H), 7.50 (d, *J* = 8.4 Hz, 2H), 4.03 (s, 1H). ESI-MS *m/z* 221.4 (M + H<sup>+</sup>)<sup>+</sup>. MW: 220.65 g/mol.

**4-(3-Chloro-2-methylphenyl)-6-((4-chlorophenyl)(hydroxy)(1-methyl-1*H*-imidazol-5-yl)methyl)-2-methoxyquinoline (7g).** A flame-dried flask was charged with a stir bar, 4.2 g (11.58 mmol) of **6g** and sealed with a rubber septum. Solid dissolved in 20 mL of anhydrous THF was added and stirred at room temperature for 10 min. The temperature was lowered to -78 °C and stirred for another 10 min. Then 5.0 mL (1.1 equiv, 6.369 mmol) of 2.5 M *n*-butyllithium was added dropwise, accompanied by a color shift to dark yellow–orange. This was allowed to stir for 20 min. A separate flask was flame-dried and charged with 2.8 g of **11c** (1.1 equiv, 6.369 mmol). This was dissolved in 55 mL of THF and added to the flask containing quinoline in three increments, rapidly dropwise over 10 min. Color shifted steadily to yellow–gold after stirring overnight and warming slowly to room temperature. The reaction was quenched by addition of 1 volume equiv of a saturated aqueous solution of NH<sub>4</sub>Cl. This was partitioned between 1 M NH<sub>4</sub>OH and CHCl<sub>3</sub>. Organic phase was collected and solvents were removed under reduced pressure to produce a foamy, white semisolid. This was purified on silica with a mobile phase consisting of MeOH/CH<sub>2</sub>Cl<sub>2</sub> 1:10 v/v to produce 3.52 g (6.91 mmol), 60% yield. TLC (CH<sub>2</sub>Cl<sub>2</sub>:MeOH 9:1 v/v): *R*<sub>f</sub> = 0.45. <sup>1</sup>H NMR (300 MHz, CDCl<sub>3</sub>, δ): 7.86 (m, 1H), 7.59 (m, 1H), 7.43 (m, 1H), 7.20 (m, 6H), 7.01 (m, 2H), 6.79 (s, 1H), 6.17 (m, 1H), 4.12 (s, 3H), 3.30 (m, 3H), 1.90 (m, 3H). ESI-MS *m/z* 504.3 (M + H<sup>+</sup>)<sup>+</sup>. MW: 504.41 g/mol.

**4-(3-Chloro-2-methylphenyl)-6-((4-chlorophenyl)(hydroxy)(1-methyl-1*H*-imidazol-5-yl)methyl)quinolin-2(1*H*)-one (8g).** **7g** (3.5 g, 6.91 mmol) was dissolved in 15 mL of THF. Then 30 mL of 6

N HCl (25 equiv) was added dropwise. The flask was fitted with a water-cooled condenser, and the mixture was stirred at 60 °C for 5 h. THF was removed by a stream of nitrogen, and the homogeneous organic phase was made basic with excess aq 1 M NH<sub>4</sub>OH and then extracted with CHCl<sub>3</sub>. The organic was collected and dried with MgSO<sub>4</sub>, and then solvents were removed at reduced pressure. Product was purified on silica with a mobile phase consisting of MeOH/CH<sub>2</sub>Cl<sub>2</sub> 1:10 v/v to produce 2.1 g (4.28 mmol) of **8g** as a white solid, 62% yield. TLC (CH<sub>2</sub>Cl<sub>2</sub>:MeOH 9:1 v/v): *R*<sub>f</sub> = 0.30. <sup>1</sup>H NMR (300 MHz, CDCl<sub>3</sub>, δ): 7.68 (m, 1H), 7.59 (m, 1H), 7.47 (m, 2H), 7.28 (m, 3H), 7.12 (m, 3H), 6.73 (m, 1H), 6.51 (m, 1H), 6.1 (m, 1H), 3.41 (m, 3H), 1.96 (m, 3H). ESI-MS *m/z* 490.4 (M + H<sup>+</sup>)<sup>+</sup>. MW: 490.38 g/mol.

**4-(3-Chloro-2-methylphenyl)-6-((4-chlorophenyl)(hydroxy)(1-methyl-1*H*-imidazol-5-yl)methyl)-1-methylquinolin-2(1*H*)-one (9g).** **8g** (2.1 g, 4.28 mmol) was added to a 100 mL flask and dissolved in 30 mL of THF. Then 487 mg (0.5 equiv, 2.14 mmol) benzyltriethylammonium chloride was added as a phase transfer catalyst. NaOH (25.5 mL 40 wt %, 120 equiv, 17.1 g) was added and allowed to stir for approximately 10 min. CH<sub>3</sub>I (375 μL, 1.4 equiv, 6 mmol) was added, and the mixture was allowed to stir overnight. The THF was removed at reduced pressure, and the product was partitioned between CHCl<sub>3</sub> and 1 M NH<sub>4</sub>OH. The product was purified on silica with a mobile phase consisting of MeOH/CH<sub>2</sub>Cl<sub>2</sub> 1:10 v/v to produce 2.0 g (3.97 mmol) of **9g** as a colorless semisolid, 59% yield. TLC (CH<sub>2</sub>Cl<sub>2</sub>:MeOH 9:1 v/v): *R*<sub>f</sub> = 0.45. <sup>1</sup>H NMR (300 MHz, CDCl<sub>3</sub>, δ): 7.80 (m, 1H), 7.72 (m, 1H), 7.63 (m, 1H), 7.49 (m, 1H), 7.29 (m, 3H), 7.12 (m, 3H), 6.78 (m, 1H), 6.58 (m, 1H), 6.14 (m, 1H), 3.85 (s, 3H), 3.41 (m, 3H), 1.95 (m, 3H). ESI-MS *m/z* 504.3 (M + H<sup>+</sup>)<sup>+</sup>. MW: 504.41 g/mol.

**4-(3-Chloro-2-methylphenyl)-6-((4-chlorophenyl)(methoxy)(1-methyl-1*H*-imidazol-5-yl)methyl)-1-methylquinolin-2(1*H*)-one (2g).** **9g** (60.0 mg, 0.119 mmol) was dissolved in 10 mL of MeOH, and approximately 60 mg of tosic acid was added. The reaction was heated to reflux for 48 h. One spot by TLC. Solvents were removed under reduced pressure to produce a colorless, oily semisolid. Product was purified by HPLC using a water–methanol gradient with 0.08% v/v trifluoroacetic acid, 30–100% over 20 min, followed by 10 min at 100%. Product elutes at 16.1 min; 56.5 mg (0.0893 mmol) produced as a mono-TFA salt. Yield 75%. TLC (CH<sub>2</sub>Cl<sub>2</sub>:MeOH 9:1 v/v): *R*<sub>f</sub> = 0.55. <sup>1</sup>H NMR (300 MHz, CDCl<sub>3</sub>, δ): 8.99 (m, 1H), 7.85 (m, 1H), 7.75 (m, 1H), 7.53 (m, 2H), 7.35 (m, 5H), 7.14 (m, 1H), 6.98 (m, 1H), 6.62 (s, 1H), 3.83 (s, 3H), 3.53 (m, 3H), 3.19 (s, 3H), 1.99 (m, 3H). ESI-MS *m/z* 518.6 (M + H<sup>+</sup>)<sup>+</sup>. MW: 518.43 g/mol. Mono-TFA salt. FW: 632.42 g/mol.

**Supporting Information Available:** Binding of key compounds to *T. cruzi* and human Lanosterol 14α-Demethylase assay; HPLC chromatogram of compound **2g**. This material is available free of charge via the Internet at <http://pubs.acs.org>.

## References

- Hucke, O.; Gelb, M. H.; Verlinde, C. L.; Buckner, F. S. The Protein Farnesyltransferase Inhibitor Tipifarnib as a New Lead for the Development of Drugs against Chagas Disease. *J. Med. Chem.* **2005**, *48*, 5415–5418.
- Sparreboom, A.; Marsh, S.; Mathijssen, R. H.; Verweij, J.; McLeod, H. L. Pharmacogenetics of tipifarnib (R115777) transport and metabolism in cancer patients. *Invest. New Drugs* **2004**, *22*, 285–9.
- Zujewski, J.; Horak, I. D.; Bol, C. J.; Woestenborghs, R.; Bowden, C.; End, D. W.; Piotrovsky, V. K.; Chiao, J.; Belly, R. T.; Todd, A. T.; Kopp, W. C.; Kohler, D. R.; Chow, C.; Noone, M.; Hakim, F. T.; Larkin, G.; Gress, R. E.; Nussenblatt, R. B.; Kremer, A. B.; Cowan, K. H. Phase I and pharmacokinetic study of farnesyl protein transferase inhibitor R115777 in advanced cancer. *J. Clin. Oncol.* **2000**, *18*, 927–941.
- Venet, M.; End, D.; Angibaud, P. Farnesyl protein transferase inhibitor ZARNESTRA R115777—history of a discovery. *Curr. Top. Med. Chem.* **2003**, *3*.
- Molina, J.; Martins-Filho, O.; Brener, Z.; Romanha, A. J.; Loeberberg, D.; Urbina, J. A. Activities of the Triazole Derivative SCH 56592 (Posaconazole) against Drug-Resistant Strains of the Protozoan Parasite *Trypanosoma* (Schizotrypanum) *cruzi* in Immunocompetent and Im-



- munosuppressed Murine Hosts. *Antimicrob. Agents Chemother.* **2000**, *44*, 150–5.
- (6) Bennett, F.; Saksena, A. K.; Lovey, R. G.; Liu, Y.; Patel, N. M.; Pinto, P.; Pike, R.; Jao, E.; Girijavallabhan, V. M.; Ganguly, A. K.; Loebenber, D.; Wang, H.; Cacciapuoti, A.; Moss, E.; Menzel, F.; Hare, R. S.; Nomeir, A. Hydroxylated analogues of the orally active broad spectrum antifungal, Sch 51048 (1), and the discovery of posaconazole [Sch 56592; 2 or (S,S)-5]. *Bioorg. Med. Chem. Lett.* **2006**, *16*, 186–190.
- (7) Saksena, A. K.; Girijavallabhan, V. M.; Wang, H.; Lovey, R. G.; F., G.; Mergelsberg, I.; Puar, M. S. Stereoselective Grignard additions to *N*-formyl hydrazones: a concise synthesis of NoxafilR side chain and a synthesis of NoxafilR. *Tetrahedron Lett.* **2004**, *45*, 8249–8251.
- (8) Saksena, A. K.; Girijavallabhan, V. M.; Lovey, R. G.; Pike, R. E.; Wang, H.; Liu, Y.; Ganguly, A. K.; Bennett, F. Tetrahydrofuran Antifungals. WO 1996/038443 A1, 1996.
- (9) Reid, T. S.; Beese, L. S. Crystal Structures of the Anticancer Clinical Candidates R115777 (Tipifarnib) and BMS-214662 Complexed with Protein Farnesyltransferase Suggest a Mechanism of FTI Selectivity. *Biochemistry* **2004**, *43*, 6877–6884.
- (10) Podust, L. M.; Poulos, T. L.; Waterman, M. R. Crystal structure of cytochrome P450 14 $\alpha$ -sterol demethylase (CYP51) from *Mycobacterium tuberculosis* in complex with azole inhibitors. *Proc. Natl. Acad. Sci. U.S.A.* **2001**, *98*, 3068–3073.
- (11) Angibaud, P. R.; Venet, M. G.; Filliers, W.; Broeckx, R.; Ligny, Y. A.; Muller, P.; Poncellet, V. S.; End, D. W. Synthesis Routes Towards the Farnesyl Protein Transferase Inhibitor ZARNESTRA. *Eur. J. Org. Chem.* **2004**, 479–486.
- (12) Frye, S. V.; Johnson, M. C.; Valvano, N. L. Synthesis of 2-aminobenzophenones via rapid halogen-lithium exchange in the presence of a 2-amino-*N*-methoxy-*N*-methylbenzamide. *J. Org. Chem.* **1991**, *56*, 3750–3752.
- (13) Venet, M. G.; Angibaud, P. R.; Muller, P.; Sanz, G. C. Farnesyl protein transferase inhibiting (imidazol-5-yl)methyl-2-quinolinone derivatives. WO 1997/021701 A1, 1997.
- (14) Venet, M. G.; Angibaud, P. R.; Muller, P.; Sanz, G. C. Farnesyl protein transferase inhibiting (imidazol-5-yl)methyl-2-quinolinone derivatives. U.S. Patent US 6037350, 2000.
- (15) Yang, B. V. Heteroaryl-substituted quinolin-2-one derivatives useful as anticancer agent. WO 2000/047574 A1, 2000.
- (16) Vejdeck, Z.; Holubek, J.; Ryska, M.; Koruna, I.; Svatek, E.; Budesinsky, M.; Protiva, M. Reactions of 4-Chloro-1-nitrobenzene with *o*-Substituted Phenylacetonitriles; Synthesis of 8-Chloro-1-methyl-(and methylthiomethyl)-6-(2-substituted phenyl)-4*H*-s-triazolo[4,3-*a*]-1,4-benzodiazepines. *Collect. Czech. Chem. Commun.* **1987**, *52*, 2545–2563.
- (17) Faller, J. W.; Lavoie, A. R. Enantioselective Syntheses of Nonracemic Benzyl- $\alpha$ -D-Alcohols via Catalytic Transfer-Hydrogenation with Ru, Os, Rh, and Ir Catalysts. *Organometallics* **2002**, *21*, 3493–3495.
- (18) Mitchell, R. H.; Lai, Y. Syntheses and Reactions of the First Dithia[3.1.3.1]metacyclophanes, [2.1.2.1]Metacyclophanes, and [2.1.2.1]-Metacyclophanes. *J. Org. Chem.* **1984**, *49*, 2534–2540.
- (19) Friedman, L.; Shechter, H. Preparation of Nitriles from Halides and Sodium Cyanide. An Advantageous Nucleophilic Displacement in Dimethyl Sulfoxide. *J. Org. Chem.* **1960**, *25*, 877–879.
- (20) Walsh, D. A. The Synthesis of 2-Aminobenzophenones. *Synthesis* **1980**, (Sept.), 677–688.
- (21) Pratt, E. F.; Draper, J. D. Reaction Rates by Distillation. I. The Etherification of Phenylcarbinols and the Transesterification of their Ethers. *J. Am. Chem. Soc.* **1949**, *71*, 2846–2849.
- (22) Araujo, M. S.; Martins-Filho, O. A.; Pereira, M. E.; Brener, Z. A combination of benzimidazole and ketoconazole enhances efficacy of chemotherapy of experimental Chagas' disease. *J. Antimicrob. Chemother.* **2000**, *45*, 819–824.
- (23) Brener, Z.; Cancado, J. R.; Galvao, L. M.; da Luz, Z. M.; Filardi, L. S.; Pereira, M. E.; Santos, L. M.; Cancado, J. R. An experimental and clinical assay with ketoconazole in the treatment of Chagas disease. *Mem. Inst. Oswaldo Cruz* **1993**, *88*, 149–153.
- (24) Bustamante, J. A.; Bixby, L. M.; Tarleton, R. L. Drug-induced cure drives conversion to a stable and protective CD8+ T central memory response in chronic Chagas disease. *Nat. Med.* **2008**, *14*, 542–550.
- (25) Corrales, M.; Cardozo, R.; Segura, M. A.; Urbina, J. A.; Basombrio, M. A. Comparative Efficacies of TAK-187, a Long-Lasting Ergosterol Biosynthesis Inhibitor, and Benzimidazole in Preventing Cardiac Damage in a Murine Model of Chagas' Disease. *Antimicrob. Agents Chemother.* **2005**, *49*, 1556–1560.
- (26) Urbina, J. A.; Payares, G.; Sanoja, C.; Lira, R.; Romanha, A. J. In vitro and in vivo activities of ravuconazole on *Trypanosoma cruzi*, the causative agent of Chagas disease. *Int. J. Antimicrob. Agents* **2003**, *21*, 27–38.
- (27) McMartin, C.; Bohacek, R. S. QXP: Powerful, rapid computer algorithms for structure-based drug design. *J. Comput-Aided Mol. Des.* **1997**, *11*, 333–344.
- (28) Yokoyama, K.; Zimmerman, K.; Scholten, J.; Gelb, M. H. Differential Prenyl Pyrophosphate Binding to Mammalian Protein Geranylgeranyltransferase-I and Protein Farnesyltransferase and Its Consequence on the Specificity of Protein Prenylation. *J. Biol. Chem.* **1997**, *272*, 3944–3952.
- (29) Van Voorhis, W. C.; Rivas, K. L.; Bendale, P.; Nallan, N.; Horney, C.; Barrett, L. K.; Bauer, K. D.; Smart, B. P.; Ankala, S.; Hucce, O.; Verlinde, C. L. M. J.; Chakrabarti, D.; Strickland, C.; Yokoyama, K.; Buckner, F. S.; Hamilton, A. D.; Williams, D. K.; Lombardo, L. J.; Floyd, D.; Gelb, M. H. Efficacy, Pharmacokinetics, and Metabolism of Tetrahydroquinoline Inhibitors of *Plasmodium falciparum* Protein Farnesyltransferase. *Antimicrob. Agents Chemother.* **2007**, *51*, 3659–3671.
- (30) Buckner, F. S.; Verlinde, C. L.; La Flamme, A. C.; Van Voorhis, W. C. Efficient technique for screening drugs for activity against *Trypanosoma cruzi* using parasites expressing  $\beta$ -galactosidase. *Antimicrob. Agents Chemother.* **1996**, *40*, 2592–7.
- (31) Van Voorhis, W. C.; Eisen, H. Fl-160. A surface antigen of *Trypanosoma cruzi* that mimics mammalian nervous tissue. *J. Exp. Med.* **1989**, *169*, 641–652.

JM801313T